

# EMITTANCE CONTROL OF A BEAM BY SHAPING THE TRANSVERSE CHARGE DISTRIBUTION, USING A TOMOGRAPHY DIAGNOSTIC

V. Yakimenko, M. Babzien, I. Ben-Zvi, R. Malone, X.-J. Wang,

National Synchrotron Light Source, Brookhaven National Laboratory, Upton, NY 11973

## Abstract

A high-brightness beam is very important for many applications. A diagnostic that measures the multi-dimensional phase-space density-distribution of the electron bunch is a must for obtaining such beams. Measurement of a slice emittance has been achieved [1]. Tomographic reconstruction of phase space was suggested [2] and implemented [3,4] using a single quadrupole scan. In the present work we give special attention to the accuracy of the phase space reconstruction and present an analysis using a transport line with nine focusing magnets and techniques to control the optical functions and phases. This diagnostic, coupled with control of the radial charge distribution of presents an opportunity to improve the beam brightness. Combining the slice emittance and tomography diagnostics lead to an unprecedented visualization of phase space distributions in 5 dimensional phase-space and an opportunity to perform high-order emittance corrections.

## 1 TOMOGRAPHIC RECOVERY

Tomography is the technique of reconstructing an object from its projections. In the Physics of beams one can use tomographic techniques to reconstruct a beam density distribution in phase space using its projections in real space. In other words, the images of a beam on a phosphorescent screen (taken, for example, by a CCD camera) can be used to derive the phase-space density-distribution. In order to do that, we must be able to rotate the distribution in phase space to generate independent projections on the screen. This is accomplished by changing the beam transport matrix in a specific way, using variable strength lenses.

In order to establish the quality of the tomographic recovery procedure, a special program based on Mathcad was developed. Some of the issues studied were the tolerances for angular or stretching errors in the focusing-channel, the required number of measured projections, the effect of smoothening during recovery and more. A special electron beam distribution with fine features (a "phantom") was chosen to simulate the recovery and compare it to the original phantom, as shown in Fig. 1. The fine structure details (tails) are on a size scale approximately 1/10 of the core.

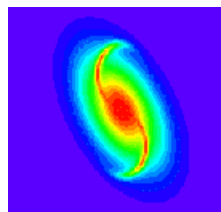


Figure 1. The Y-Y' phase space distribution of the phantom.

The phantom distribution is propagated through the accelerator using a transport matrix to the location of the beam monitor, where the projection is generated numerically and saved as a "measurement". The "measured" projections are used to reconstruct the original distribution and then compared with the phantom to establish the quality of the tomographic reconstruction. This is a standard tomography technique.

The effects of the number of projections are presented in Fig. 2. Fig. 2a represents a recovery using 32 "measured" projections equally spaced over 180 degrees. In Fig. 2b the recovery is done with only 16 "measured" projections. It is possible to generate artificial projections by interpolation of measured projections during analysis. The recovery using 16 "measured" projections plus 16 interpolated projections (32 total) is presented in Fig. 2c. We reach the qualitative conclusion that to be able to detect distribution details at one tenth of the core, the number of measured projections should be between 16 to 32 without using any interpolations.

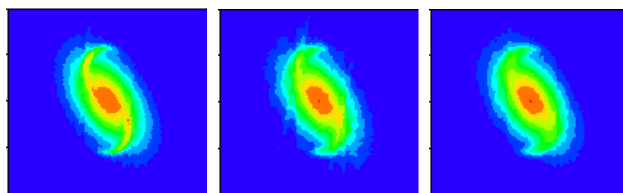


Figure 2. Y-Y' plane tomographic recovery of the phantom phase space distribution using different numbers of "measured" and interpolated projections. From left to right: a. 32 projections, b. 16 projections, c. 16 projections and 16 interpolations.

Next, we determined the required accuracy in the determination of the phase rotation angle and the transversal stretching of the phase space distribution produced by the beam matrix. Fig. 3 illustrates the

recovery of the phantom distribution using 32 "measured" projections, with: a. 10% simulated RMS error in phases; b. 10% simulated RMS errors in transversal stretching; c. 10% phase and 10% stretching. We conclude that the rotation phase error should be of the order of 10%.

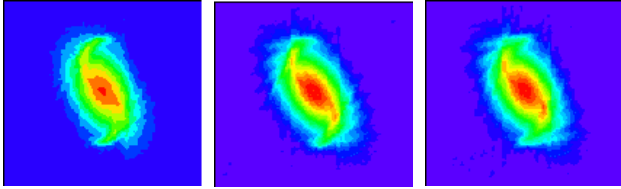


Figure 3. Y-Y' tomographic recovery of the phantom phase space distribution using simulated angular and scale errors. From left to right: a. 10% phase error; b. 10% stretch error; c. combined 10% phase and 10% stretch errors.

## 2 THE EXPERIMENTAL SETUP

The electron beam is produced by laser photocathode RF gun. A linear emittance compensation solenoid is located right after the RF gun controls the phase space distribution of the electron beam. Two RF linac sections with independent phase control accelerate beam from 5 MeV to approximately 50 MeV. A long beam line, immediately downstream of the linac, is used to generate rotations (phase advance) without a change in the beam size (constant optical functions). This beam line section has 9 quadrupole lenses as well as four beam profile monitors. Thus a complete control of the horizontal and vertical machine functions and satisfactory degree of monitoring are possible. A high-quality beam profile monitor at the end of this line (just before a dipole magnet) was used to measure the projection. The recovery procedure determines the phase space distribution at the first beam profile monitor following the linac.

The tomographic reconstruction of transverse phase space may be combined with the measurement of a longitudinal slice [1], to produce the transverse phase space distribution of a longitudinal slice [4]. This leads to a measurement of the 5 dimensional phase space density distribution in  $(X, P_x, Y, P_y, Z)$ . For this purpose we introduce a linear energy chirp by de-phasing the second linac section and then select a longitudinal slice of the beam by a slit, located in the dispersive beam line downstream of the dipole. Tomographic measurements of a slice may be done at a beam profile monitor, located downstream of the slit, in the (non dispersive) Y-Y' plane. Alternately, a measurement of both X-X' and Y-Y' is possible in one of the experiment hall dispersion free beam lines downstream of another dipole.

## 3 THE COMPUTER CONTROL SYSTEM

The beam tomography application uses three subsystems of the Accelerator Test Facility's computer network: 1) the main control system and its peripherals, 2) a PC-based video frame grabber and 3) an additional PC on which the tomography application code resides.

**The central control computer** is a Digital VAX 4200 configured with a serial highway. Six CAMAC crates are located at several positions around the complex, each equipped with interface cards to control and monitor the facility's various devices, including magnetic optics components and beam diagnostics. Host to crate communication takes place over the serial highway. The operating system is Open VMS with TCP/IP network support. Vsystem, a commercial software tool package, is used to construct operator displays, generate the underlying database and provide an interface for applications programs. In addition to the main system, other computers are networked over a local area Ethernet.

**PC-based Video Frame Grabber:** Video frame analysis is the primary measurement technique used in this application. A PC-based frame grabber system was built using components, including a video motherboard, a variable scan video acquisition, 8-bit digitizer and a series of computation modules, resulting a high-performance, pipelined video image processor occupying 2 PCI slots. Most computations and projections are developed locally in this dedicated arithmetic hardware where all modules can communicate over their own local bus, thus placing no serious burden on the host PC. Frame grabbing, digitization and display are all completely synchronous with each pulse of the electron beam. Programming to control this subsystem was done using Microsoft Visual C++ under Windows NT. It can operate either as a stand-alone instrument (setup and results displayed on a local monitor) or as a slave device where commands and data are exchanged over a network TCP socket connection.

**The tomography computer** holds and executes all the actual logic needed to carry out a measurement. Like the frame grabber PC, it was also programmed using Visual C++ under Windows NT. Its program, called "TOMO", orchestrates the step-by-step actions needed to complete a measurement sequence, directing the main control VAX to manage facility hardware on its behalf. Once authorized, the tomography application has complete access to the accelerator database. By sending and receiving socket messages, values can be written to or read from the database, in turn signaling detached server processes to implement the desired action. These messages and acknowledgements mimic the actions a human operator would follow in making a measurement: setting and verifying magnet current, inserting and retracting beam profile monitors, switching video

cameras to the frame grabber, requesting image statistics and projections, etc.

The tomographic measurement can be broken into a few steps.

1. The first step of the tomographic analysis is a measurement of the initial conditions of the electron beam at the linac's exit. The variation of the beam size as a function of current in the first triplet is used to match the optical functions in two directions.
2. In the second step, we calculate tunes for the just-measured initial conditions of the beam. A simplex method is used to match the required phase advance and keep the electron-beam conditions at the end of the transport line nearly constant.
3. The third step is to measure the beam projections for the tunes calculated in the previous step.
4. In the last step we reconstruct the phase space distribution from the measured projections.

#### 4 EMITTANCE CONTROL

Shaping the photocathode RF gun's laser intensity profile shapes the electron beam charge distribution. This may lead to non-linear emittance corrections and to possible improvements in the brightness of electron guns.

Normal beam propagation in laser systems consists of Gaussian or near Gaussian profiles. Other profiles can be derived from this in a number of ways. A more uniform profile can be achieved by expanding the Gaussian beam and cutting the tails of the distribution with an iris diaphragm. A final and only slightly more complex case is to place a central obstruction in the beam path in combination with the iris to produce the annular profile.

These three profiles were used in the electron-beam tomography-measurements. In the following three figures (Figs. 4,5,6) we present the laser transverse distribution (on the left) and tomographic recovery of the electron beam phase space (on the right) for the three laser intensity distributions described above. The laser spot diameter in Fig. 5 (nearly uniform laser distribution) is 2 mm. The laser intensity is adjusted to provide the same beam charge, which is 0.5 nano-Coulomb for the three laser distributions. The tomographic recovery is in the vertical plane ( $Y-Y'$ ) and the units are such that the full size (edge to edge) of each figure is 7 mm in  $Y$  and 0.7 mrad in  $Y'$ .

The phase space density distributions in Figs. 4,5,6 display beam halos. At this point we are not sure if these are the result of a real halo or an artifact of the reconstruction. The photocathode gun laser parameters (phase and amplitude) may have changed somewhat from one projection measurement to the next. This may affect slightly the beam transport through the system and thus the quality of the reconstruction. Stability is extremely important in such measurements.

The tomographic analysis demonstrates clearly that the distribution with increased flatness presents the best beam brightness (the smallest area in transverse phase space) of the three measured distributions. The beam intensity used in these measurements (0.5 nC) produces some phase space distortion, even in the nearly flat radial charge distribution (Fig. 5). In future experiments we will study higher beam charges and attempt to correct the emittance by modifying the charge distribution. This will be a non-linear transverse emittance correction.

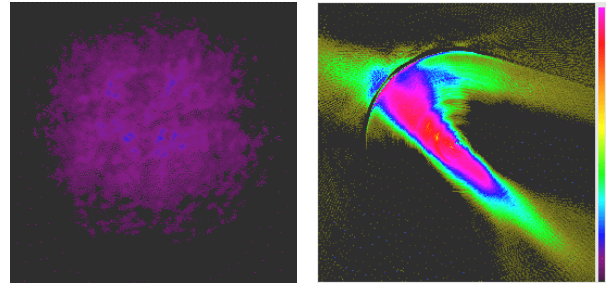


Figure 4. From left to right: a. Gaussian laser intensity profile; b. The tomographic recovery of the electron beam's transverse phase space.

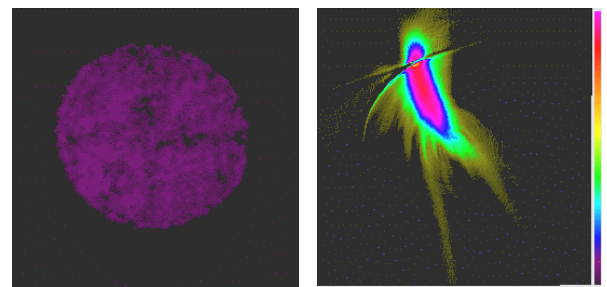


Figure 5. From left to right: a. Increased flatness laser intensity profile; b. the tomographic recovery.

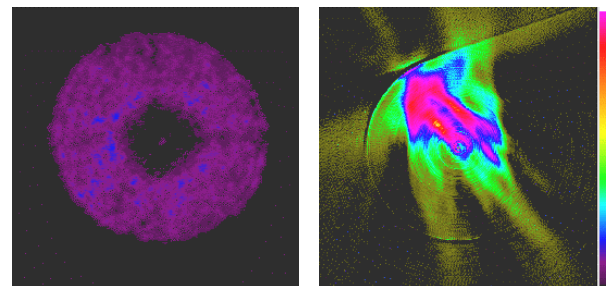


Figure 6. From left to right: a. the "Donut" laser intensity profile; b. the tomographic recovery of the electron beam's transverse phase space.

#### 5 REFERENCES

- [1] X. Qiu, K. Batchelor, I. Ben-Zvi and X.J. Wang, *Phys. Rev. Lett.* **76** No. 20, 3723, (1996)
- [2] J.S. Fraser, *IEEE Trans. Nucl. Sci.* NS-26, No. 1, 1641 (1979)
- [3] C.B. McKee, P.G. O'Shea and J.M.J. Madey, *Nucl. Inst. And Meth. In Phys. Res.* A358, 264 (1995)
- [4] I. Ben-Zvi, J.X. Qiu and X.J. Wang, *Proc. PAC'97, Vancouver BC Canada, May 12-16, 1997*